ISSN: 2277-9655
Impact Factor: 5.164
CODEN: IJESS7

IJESRT
INTERNATIONAL JOURNAL OF ENGINEERING SCIENCES & RESEARCH TECHNOLOGY

STRUCTURAL, OPTICAL AND PHOTO CATALYTIC PROPERTIES OF PVP ENCAPSULATED Ni^{2+} Substituted ZnS NANOPARTICLES BY MODIFIED CO-PRECIPITATION METHOD

G. Vijayakumar[1], G. Bhoopathi[*2], Jude Leonard Hilary[3]
[1 & *2] Department of Physics, PSG College of Arts and Science, Coimbatore – 641 014
[3] Department of Physics, St.Joseph's College of Arts and Science, Cuddalore – 607 001

DOI: 10.5281/zenodo.1189044

ABSTRACT
In the present work, PVP encapsulated ZnS:Ni nanoparticles were prepared through modified chemical precipitation method using oxalic acid precursor. The structural and optical properties of the prepared samples were characterized using X-ray diffraction (XRD) studies and UV–Vis-NIR Spectrophotometer. Morphological and chemical properties were studied carried out using Scanning Electron Microscopy (SEM) and Energy Dispersive Analysis of X-rays (EDAX). XRD pattern analysis confirms the zinc blende structure of pure ZnS and PVP encapsulated Ni doped ZnS nanoparticles with the crystallite size of 10 nm. The optical band gap has been found to be in the range 4.2- 3.9 eV. Room temperature photoluminescence (PL) spectrum of the undoped sample exhibits emission in the blue region with multiple peaks under UV excitation. The degradation of methyl orange (MO) under visible light irradiation was carried out to study the photocatalytic activity of the prepared samples. It was found that the sample 0.5% Ni substituted ZnS exhibited the higher photocatalytic activity due to higher initial saturation value under UV irradiation for 15 min.

KEYWORDS: Ni doped ZnS; Modified co-precipitation; Photocatalysis; Azo dyes

I. INTRODUCTION
Compound semiconductors have attracted considerable technological and scientific interest due to their large range of electronic energy band gaps. There are generally eight II-VI compound semiconductors ZnO, ZnS, ZnSe, ZnTe, CdO, CdS, CdSe and CdTe, which are widely recognized. Among these materials, ZnS has been realized to be the potential candidate for extensive research, possible applications in optoelectronics and the potential generalization of results to other nanomaterials. ZnS is a wide band gap material with band gaps of 3.68 eV (zincblende) and 3.91eV (wurtzite) [1]. It displays a high refractive index of 2.2 and high transmittance of light in the visible region of the spectrum. These properties make ZnS a strong candidate for optoelectronic devices. In recent years, nanocrystalline ZnS has been reported to have some characteristics, different from the bulk properties, which may extend its application range. Therefore, much attention has been focused on the synthesis of ZnS nanoparticles and films, and the exploration of their novel properties. Several approaches are available to obtain nanocrystalline ZnS. It offers the advantages of wide energy band gap, higher optical transmittance, low cost and abundancy of the constituent elements that are less toxic and tunability of the energy band gap, lattice parameter and electron affinity by the addition of suitable dopant that could be perfectly matched with the absorber material, with a band gap between 1.3 eV and 1.6 eV. Therefore, it is worth to investigate undoped and doped ZnS as an alternative buffer/window layer to CdS. ZnS is a potential candidate for device applications because of its wide band gap, large exciton binding energy (40 meV), high index of refraction (2.27 at 1 μm) and has been identified as an excellent host semiconductor for supporting room temperature ferromagnetism when doped with a variety of 3d transition metal ions [2]. The three primary dopant metals Fe, Co and Ni are ferromagnetic at room temperature. Ionic radii of these dopants (Co^{2+}= 0.65 Å, Ni^{2+}= 0.69 Å and Fe^{2+}= 0.63 Å) are smaller than that of Zn^{2+} (0.74 Å). Hence these replace Zn2+ in the host lattice. ZnS an excellent host and Fe, Ni as dopants in low concentrations have been identified to have good prospects of producing room temperature ferromagnetism (RTFM). Semiconductors and magnetic materials are two very

ISSN: 2277-9655
Impact Factor: 5.164
CODEN: IJESS7

important classes of materials in the current electronic industries [3]. By combining these two types of materials a new class of materials, displaying both the semiconducting as well as the magnetic properties, is formed. These materials are known as 'diluted magnetic semiconductors (DMS). Electronic devices fabricated with DMS materials display enhanced efficiencies. Diluted magnetic semiconductors (DMS) are compound semiconductors, in which a part of the nonmagnetic cations of the host material has been randomly substituted by magnetic ions like transition metals or rare earth metals. Transition metals that have partially filled d states (Sc, Ti, V, Cr, Mn, Fe, Co, Ni, Cu) and rare earth elements that have partially filled f states (e.g. Eu, Gd, Er) have been used as substituent magnetic atoms in DMS. Among the II-VI semiconductor group materials, ZnS has been realized to be the potential candidate for extensive research, possible applications in optoelectronics and the potential generalization of results to other nanomaterials. ZnS is a wide band gap material with band gaps of 3.68 eV (zincblende) and 3.91eV (wurtzite). It displays a high refractive index of 2.2 and high transmittance of light in the visible region of the spectrum [4]. These properties make ZnS a strong candidate for optoelectronic devices. Present study focuses on the investigation on the structural, optical and magnetic properties of PVP encapsulated ZnS:Fe/Ni nanoparticles synthesized by the chemical precipitation method.

II. MATERIALS AND METHODS

2.1 Materials

Zinc acetate dihydrate, Nickel acetate tetrahydrate, oxalic acid, poly vinyl pyrolidone (PVP) were purchased from Merck, India. The chemical reagents were of analytical reagent grade and were used without further purification. All the glasswares used in this experimental work were washed with deionized water and dried in oven.

2.2 Preparation of PVP encapsulated Ni doped ZnS nanoparticles

Nanocrystalline Ni^{2+} ions doped ZnS nanoparticle was synthesized through oxalic acid based precursor method. Ethanol was used as solvent for all the stages of experiment. Zinc acetate dihydrate (0.5 M) and nickel acetate tetrahydrate (0.5, 1.0 & 1.5 %) are dissolved together in 60 ml of deionized water and stirred for 30 min. The obtained aqueous solution was mixed with oxalic acid in 1:3 molar ratio. 0.5g of polyvinyl pyrolidone (PVP) was dissolved in 50 ml of de-ionized water and was stirred to dissolve completely. Equimolar ratio of oxalic acid mixture and PVP solution were added and was stirred for 30 minutes. The concentration of Ni^{2+} in ZnS was adjusted by controlling the amount of nickel acetate added in the above mixture. This solution was then stirred in argon atmosphere keeping the temperature at 80 °C for one hour. To this solution, aqueous solution of sodium sulfide (0.5 M) was added drop-wise until the observation of sufficient white precipitate due to the formation of ZnS:Ni^{2+} nanoparticles under stirring for 30 min at 80 °C.

2.3 Characterization techniques

The samples were characterized by X-ray diffraction (XRD) using a D8 BRUKER AXS diffractometer with Cu Kα, operating at 40 kV and 30 mA. Doping of Ni in ZnS was confirmed by energy dispersive x-ray (EDX) spectroscopy using NORAN System Six. Size and surface morphology of the samples were studied through JEOL (JXA-8200) scanning electron microscopy (SEM). Perkin Elmer (350) UV-Visible spectrophotometer was used to record optical absorption spectra and, Cary Varian fluoro-spectrophotometer, to measure PL.

2.4 Photocatalytic degradation

A 200 ml reagent beaker was used as the reactor for the study. The illumination was provided with 15 W compact fluorescent lamp (CFL). To study photocatalytic activity, a known concentration of the catalyst (ZnS:Ni) was dispersed in methyl orange dye. This solution was first placed in dark for one hour to reach a state of adsorption equilibrium, and, then, illuminated with a visible-light source of 10,000 lux. The absorption peak from 450 to 500 nm was monitored to carry out degradation analysis of ZnS:Ni.

III. RESULTS AND DISCUSSION

3.1 Elemental analysis

The energy dispersive X-ray analysis (EDAX) spectra of the pure ZnS and PVP encapsulated ZnS:Ni^{2+} are shown in the Figure below. The spectral signals from Fig.1.1 and Fig.1.2 confirms the presence of Zn, S and Ni indicating that the prepared nanoparticles constitute zinc, sulphur and nickel dopant only and no other impurity atoms. The chemical constituents present in the sample according to the EDAX results were listed in the table1 below.

ISSN: 2277-9655
Impact Factor: 5.164
CODEN: IJESS7

Table.1 Elemental Composition

Composition		
Zn	**S**	**Ni**
50.53	48.48	0.99
49.63	48.54	1.83
48.31	48.77	2.92

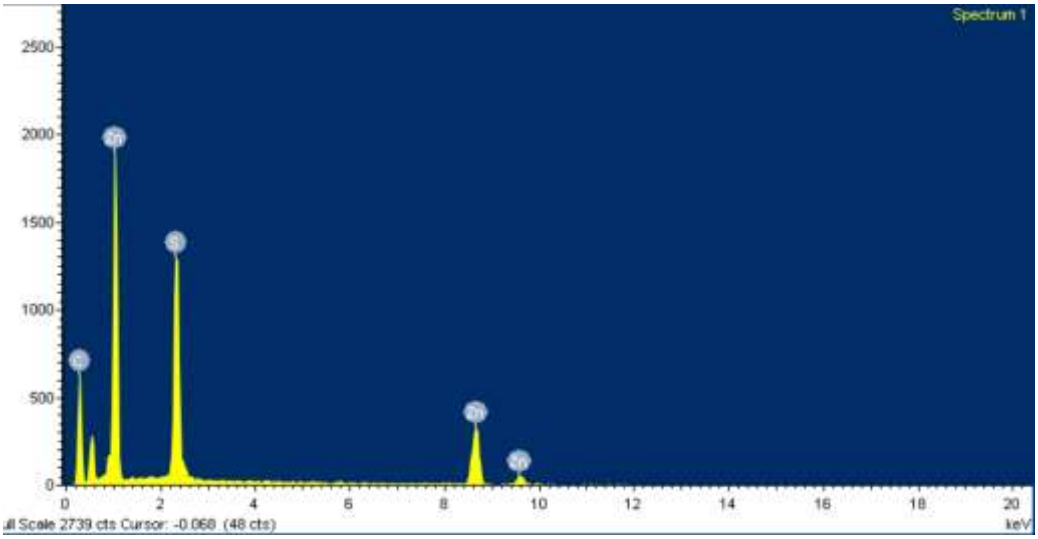

Fig.1.1 EDAX spectra of undoped ZnS nanoparticles

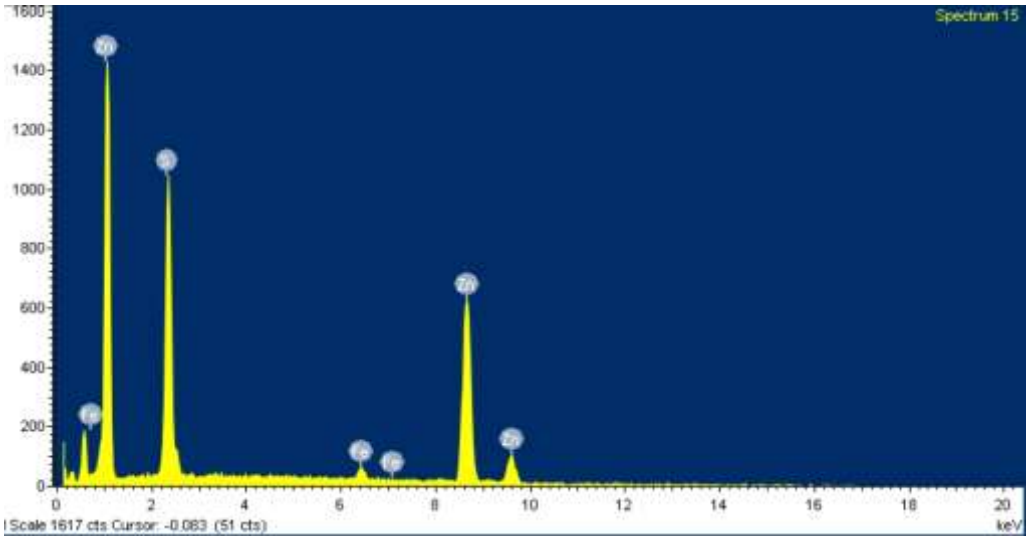

Fig.1.2 EDAX Spectra of of ZnS:Ni2+ (0.5, 1.0, 1.5%) nanoparticles

ISSN: 2277-9655
Impact Factor: 5.164
CODEN: IJESS7

3.2 Structural analysis

The XRD spectra of pure ZnS and PVP encapsulated Zns:Ni^{2+} samples at different dopant concentrations are shown in Fig 2. The diffraction peaks at 2θ ranging from 28.8°, 47.15° and 56.85° are indexed as (111), (220) and (311) planes corresponding to the Ni substituted ZnS nanoparticles respectively. The indexed peak positions matches well with the standard JCPDS file No: 65-4586 for all samples. Noise peas corresponding to secondary phases or metal clusters were not observed. The broadening of the diffraction peaks indicates the nano size of the synthesized particles. The average particle sizes for the ZnS:Ni^{2+} was estimated using the Debye-Scherrer formula from the major diffraction peak (111), lie in the range of 3.5 – 4.8 nm. The particle size decreases with increasing dopant concentration. This is because, the ionic radius of Zn^{2+} (74 r.pm) and that of Ni^{2+} ion (70 r.pm) are almost equal and the ionic radius of the dopant affects the sintering properties of the samples which in turn alters the microstructure of the samples. In addition the peak positions shift towards higher values of 2θ which results in lowering of lattice parameter with increasing Ni concentration due to the lattice contraction occurring because of the higher surface to volume ratio [5 - 10]. The calculated lattice parameter values were calculated and have been tabulated below.

Table.2 Lattice parameter corresponding to various dopant composition.

Material	Crystalline size (nm)	Lattice constant (Å)
Pure ZnS	3.8	5.40
ZnS + Ni (0.5%)	2.6	5.379
ZnS + Ni (1.0%)	2.3	5.358
ZnS + Ni (1.5%)	2.1	5.332

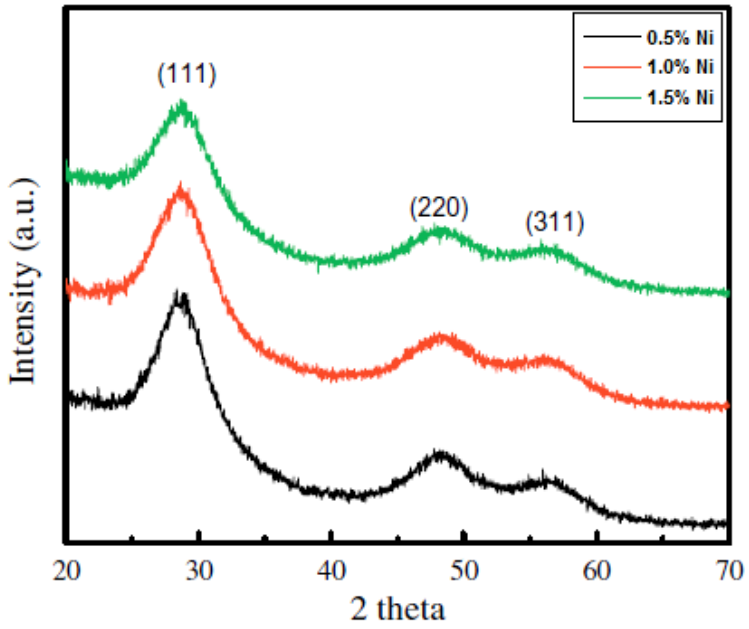

Fig.2 X-ray diffraction pattern of Ni doped ZnS Nanoparticles

The particle size was calculated using Debye-Scherrer formula and the average crystallite size of the ZnS:Ni nanoparticle lie in the range of 3.8 – 2.1 nm. This implies that the crystallite size decreases on increasing the Ni concentration on the ZnS site. The band gap energy of the Ni doped ZnS are 3.92, 3.86, 3.80,and 3.76 eV for 0.5, 1.0 and 1.5% of Ni respectively. It can be seen that the band gap decreases with the subsequent increase in

ISSN: 2277-9655
Impact Factor: 5.164
CODEN: IJESS7

the dopant concentration [11]. This effect may be due to the overlapping of host electron wave-functions with the dopant atoms. On increasing the concentration of the impurity atoms, this overlapping raises subsequently resulting in the formation of energy band rather than discrete energy levels. This impurity band formation of the dopant electron reduces the band gap energy of the parent material.

3.3 SEM

Scanning electron microscopy (SEM) is a powerful tool to study the surface morphology by observing the individual crystallites and quantification of the size and shape of the as prepared samples. Fig.3 shows the SEM images of Pure ZnS and PVP encapsulated ZnS:Ni (0.5 1.0 and 1.5%) nanoparticles respectively. From the SEM images, it can be seen that particles are slightly agglomerated in the pure ZnS nanoparticle which may be attributed to the resultant attractive forces caused by the cation concentration on the surface of the nanocrystalline system [12].

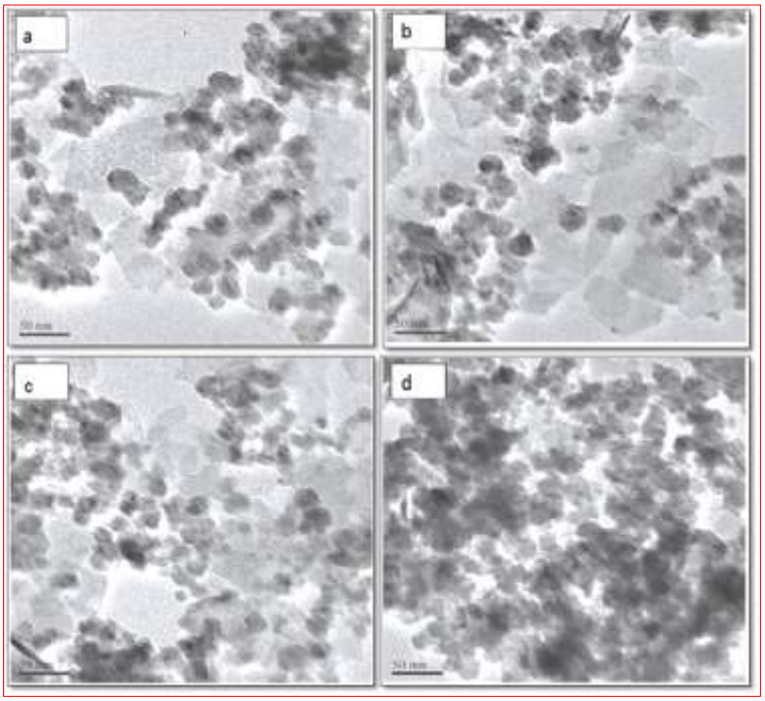

Fig.3 SEM image of (a) Pure ZnS (b) 0.5% Ni (c) 1.0% and (d) 1.5% Ni doped ZnS nanoparticle capped with PVP

SEM images of the pure ZnS and PVP capped ZnS:Ni reveals more or less uniform size particles ranging from 4.04 nm to 3.43 nm which are in good agreement with the XRD results. The PVP encapsulated ZnS:Ni^{2+} nanoparticles show spherical with homogeneous size distribution. This implies that the rapidly formed ZnS:Ni^{2+} clusters were immediately surrounded by the PVP surfactant [13]. As a result the particles were isolated. But the uncapped nanoparticle show irregular shape. This may be due to the uncontrolled growth in the absence of the capping agent. Furthermore, the above results depict that increasing molar concentration of the capping agent reduces the particle size appreciably.

3.4 UV-Vis absorption analysis

The optical absorption spectra of the undoped and Ni-doped ZnS nanoparticles encapsulated with PVP are shown in Fig.4. Optical absorption studies show that the absorption edge the shifting of absorption edge towards blue region with respect to bulk samples of ZnS indicates increase in effective band gap energy with decreasing particle size. The observed blue shift in the excitation wavelength is attributed quantum confinement effect with respect to bulk materials of these compositions.

ISSN: 2277-9655
Impact Factor: 5.164
CODEN: IJESS7

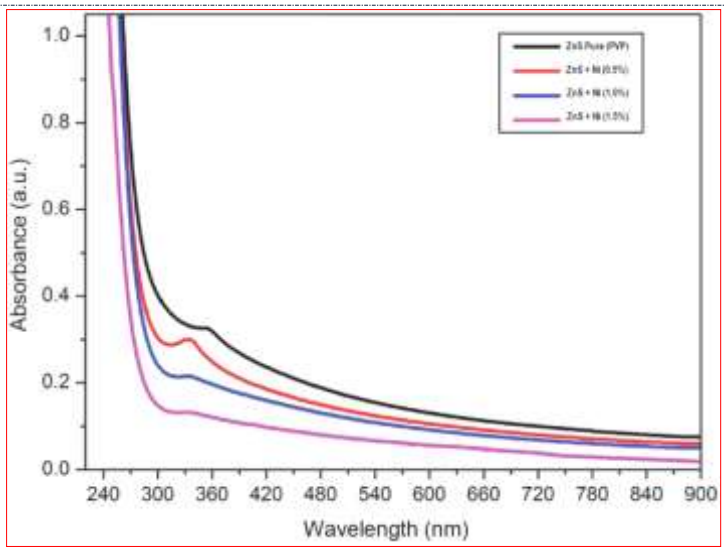

Fig.4 UV–Vis absorption characteristics of pure ZnS and ZnS:Ni nanoparticles

A sharp absorption peak was observed at 355 nm in the UV-Vis spectrum of the uncapped ZnS nanoparticles, indicating the red shift of 10 nm compared with the absorption peak of 345 nm for bulk ZnS material. However, the UV-Vis absorption spectra for the pure and PVP-encapsulated ZnS nanoparticles were highly blue shifted compared with the uncapped ZnS nanoparticles and the bulk ZnS material [14]. This magnificent shift was the consequence of the quantum size effect, which indicated a change in band gap along with exciton features that can be used as a measure of particle size and size distribution. From the plot, all the three dopant concentrations demonstrate strong blue shift in absorption region as an indication of nanophase formation and further it is observed that absorption intensity increases with increasing dopant concentration from 0.5 to 1.5 M. The blue shifts in the position of the absorption edges signify the nanophase formation and the diminishing intensity infers the non monotonic shifts, because of local (sulfur) vacancies in the crystal structure [15-18]. The sharp absorption peak was observed at 355 nm in the UV-Vis spectrum of the uncapped ZnS nanoparticles, indicating the red shift of 10 nm compared with the absorption peak of 345 nm for bulk ZnS material.

3.5 Photoluminescence study

The photoluminescence spectra of pure ZnS and PVP encapsulated ZnS:Ni nanoparticles with an excitation wavelngth of 320nm are shown in the Fig5. Both pure and doped ZnS samples exhibit broad and asymmetric peaks. The peaks of PVP encapsulated ZnS:Ni nanoparticles are flat covering the wavelength region (390-520 nm) and indicate that they comprise different emission peaks. The fluorescence capability of the PVP encapsulated ZnS:Ni nanoparticles were significantly higher than those of the undoped ZnS nanoparticles. However, on increasing the dopant concentration further the intensity of the samples with higher dopant concentration decreased [19]. From the graph it can be seen that ZnS doped with 1.0% Ni exhibits maximum PL intensity. The intensity of 1.5% Ni doped ZnS showed less intensity. This effect can be explained as the quenching phenomenon which may be due to the enlargement of non-radiative transition at higher concentartion of Ni^{2+} ions. Photoexcited electrons are transferred to large number of trapping centers induced by the nickel ions compared to anion vacancy defect centres. In the present work, similar phenomenon was observed for the PVP encapsulated ZnS:Ni nanoparticles. The photoexcited electrons are transferred to the trapping centres which act as non-radiative recombination centers thereby reducing the emission intensity. On increasing the dopant concentration, the peaks were attributed towards red shift which confirms the formation of trap states. Due to these large number of induced trap states, whenever an electron makes a transition, a negligible quantity of energy has only been transmitted to the nearest atom or lattice site [20]. As a result, the amount of energy emitted reduces considerably thereby shifting the peaks towards longer wavelength. Thus it can be concluded form the above theory that the optimized doping level for enhancing the PL intensity of PVP encapsulated Ni doped ZnS is 1%. The observed result implies the potential application of these materials in luminescent devices.

ISSN: 2277-9655
Impact Factor: 5.164
CODEN: IJESS7

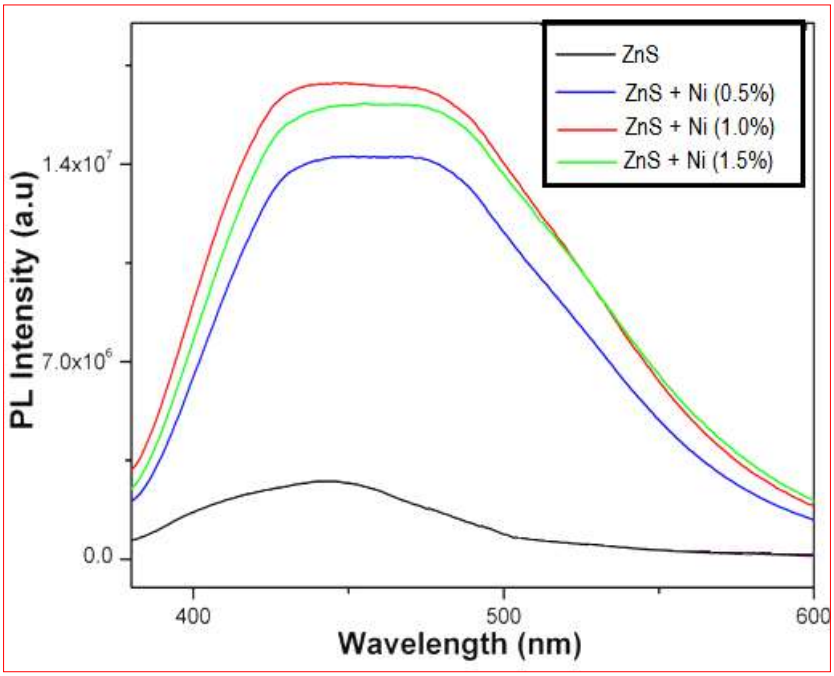

Fig.5 PL emission from pure ZnS and PVP capped ZnS:Ni nanoparticles.

3.6 Photocatalytic activity

The photodegradation of Methyl orange dye was analyzed to study the photocatalytic activity of Pure ZnS and PVP encapsulated ZnS:Ni nanopartciles. Degradation parameters such as total reaction time, concentration of the dye and amount of catalyst required were analysed to optimize the appropriate photocatalytic activity requirements. Fig.6 shows the absorption spectra of time-dependent Methyl Orange aqueous solution exposed under visible light at around 460 nm. Fig.7 shows the degradation factor of methyl orange for the reaction period of 15mins in the presence of pure and PVP encapsulated ZnS:Ni nanoparticles.

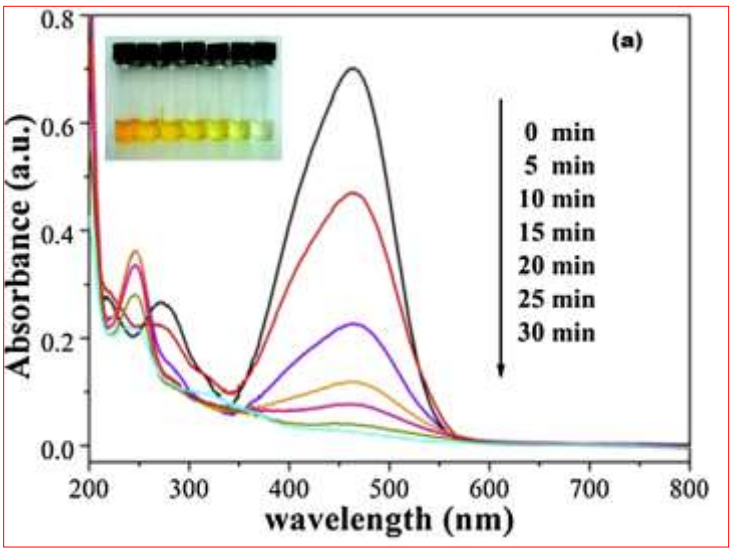

Fig.6 UV–vis absorption spectral changes of Methyl Orange by using Ni^{2+} substituted ZnS nanoparticles. The color-change sequence in the sample with irradiation times are shown in inset picture.

ISSN: 2277-9655
Impact Factor: 5.164
CODEN: IJESS7

The graph reveals that the degradation processes were less and very slow for different Ni concentrations. This may be attributed to the effective surface area and the dispersion stability of ZnS that determine the photocatalytic activity of Ni doped ZnS in methyl orange dye [21]. The effective surface area of ZnS nanoparticle decreases with the increasing concentration of the Ni2+ ions which in turn reduces the photodegradation capability of ZnS. From this result, it can effectively be formulated that ZnS nanoparticle doped with highest concentration of Ni (1.5%) shows lowest adsorption of methyl orange dye and its initial saturation value is very low compared to other concentrations [22-26].

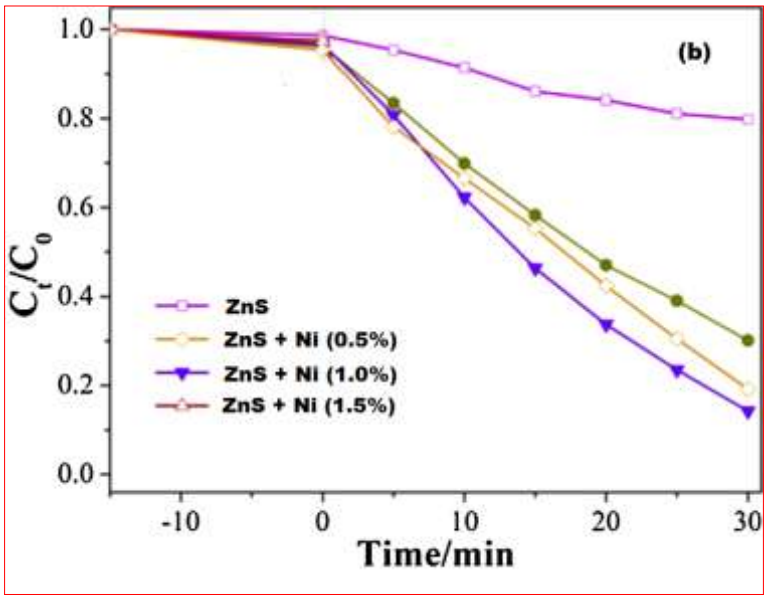

Fig.7 Results of photocatalytic degradation of MO using Ni^{2+} doped ZnS catalyst under visible light irradiation.

The next factor affecting the photodegradation process is the dispersion stability of ZnS nanoparticle. The dispersion stability of ZnS decreases with the addition of Ni^{2+} ions which reduces the effective surface area of ZnS nanoparticle resulting in low dye degradation of methyl orange [28]. Thus form the above result it can be implied that higher the Ni concentarion in the ZnS sites, lesser is the effective surface area of ZnS available for reaction in the Methyl orange zone and lower is the degradation of the chosen dye. In our study, 0.5% Ni substituted ZnS nanoparticle had higher initial saturation value due to lower Ni2+ ion content compared to 1.0% and 1.5% Ni substituted ZnS nanoparticles. Thus, the present results offer nickel as the effective dopant for the decreased photocatalytic activity of ZnS.

IV. CONCLUSION

Nanoparticles of pure and PVP encapsulated ZnS:Ni (0.5%, 1.0% and 1.5% of Ni) have been successfully synthesized by modified co-precipitation method using oxalic acid as the precursor. The encapsulated ZnS:Ni^{2+} nanoparticles showed better dispersion as they were adsorbed on the surface of nanoparticles so as to overcome the steric effect between nanoparticles and prevent agglomeration. The structural, optical, and photocatalytic properties of ZnS are significantly changed after the incorporation of Ni^{2+} ions in the ZnS lattice site. The XRD result confirms the zinc blende (cubic) structure of Ni doped ZnS nanoparticles without forming secondary phases. The particles have uniform size distribution of approximately 3.5-4.8 nm. The morphological investigation shows the nanophase formation of the as prepared samples with average particle size ranging from 4.04 to 3.43 nm. The photocatalytic analysis reveals that, among the different ratio of Ni^{2+} substituted ZnS nanoparticle, 0.5% Ni substituted ZnS exhibited excellent degradation activity of Methyl orange dye due to the increased Ni surface states in ZnS. The degradation efficiency of 0.5% Ni doped ZnS reaches 97% under UV irradiation for 30 min, which may originate from the small size with big specific area of the sample. The present study demonstrates that minimum quantities of Ni^{2+} ions are sufficient enough to stimulate photocatalytic activity of ZnS considerably. Surface modification of ZnS:Ni^{2+} nanoparticles with biocompatible substitutes are can serve as fluorescent probes for biological and medicinal applications such as targeted drug delivery.

ISSN: 2277-9655
Impact Factor: 5.164
CODEN: IJESS7

V. REFERENCES

[1] A. Tiwari, S. A. Khan, R. S. Kher, Adv. Appl. Sci. Res. 2, 105 (2011).
[2] M. Godlewski, E. Guziewicz, K. Kopalko, G. Luka, M. I. Lukasiewicz, T. Krajewski, B. S. Witkowski, S. Gieraltowska, Low Temp. Phys. 37, 235 (2011).
[3] R. E. Pimpinella, A. M. Mintairov, X. Liu, T. H. Kosel, J. L. Merz, J. K. Furdyna, M. Dobrowolska, J. Vac. Sci. Technol. B 29, 1 (2011).
[4] N. Saravanan, G. B. Tec, S. Y. P Yap, K. M. Cheong, J. Mater. Sci. Mater. Electron. 19, 1206 (2008).
[5] M. J. Pawar, S. D. Nimkar, P. P. Nannukar, A. S. Tale, S. B. Deshmukh, S. S. Chaure, Chalcogenide Letters 7, 139 (2010).
[6] W. Q. Peng, S. C. Qu, G. W. Cong, Z. G.Wang, Cryst. Growth Des. 6, 1518 (2006).
[7] S. K. Mehta, S. Kumar, S. Chaudhary, K. K. Bhasin, M. Gradzielski, Nanoscale Res. Lett. 4, 17 (2009).
[8] M. P. Anil, S. G. Shivram, J. Crystal Growth, doi:10.1016/j.jcrysgro.2011.01.087 (2011).
[9] L. Q. Yue, F. J. Zhang, J. Z. Huang, L. W. Wang, J. Nanosci. Nanotechnol. 8, 1199 (2008).
[10] R. Maitya, U.N. Maitia, M.K. Mitrab, K.K. Chattopadhyaya, Physica E 33, 104 (2006).
[11] G. Buxbaum, G. Pfaff, Industrial Inorganic Pigment, 3rd edn. WILEY-VCH, Weinheim (2005).
[12] A. Pourahmad, Spectrochim. Acta Part A 103 (2013) 193–198.
[13] L.X. Yin, D. Wang, J.F. Huang, L.Y. Cao, H.B. Ouyang, J.P. Wu, X. Yong, Ceram. Int.41 (2015) 3288–3292.
[14] K. Chakrabortya, S. Chakrabartya, P. Dasb, S. Ghosha, T. Pal, Mater. Sci. Eng. B204 (2016) 8–14.
[15] W.B. Bai, L.F. Cai, C.X. Wu, X.Q. Xiao, X.L. Fan, K.Z. Chen, J.H. Lin, Mater. Lett. 124(2014) 177–180.
[16] L.L. Chai, W. He, L. Sun, F. Jin, X.Y. Hu, J.L. Ma, Mater. Lett. 120 (2014) 26–29.
[17] Culity B. D, Elements of X-Ray Diffraction, 2nd ed., Addison Wesley, Reading mass 1956. ISBN 13: 9780201012309.
[18] Kulkarni S. K, Encyclopedia of Nanoscience and Nanotechnology, Edited by H.S. Nalwa, USA, 2 (1) 2004, pp. 537-564.
[19] Jayanthi.K, Chawla. S, Sood K.N, Chhibara M, Singh S, J.Appl.Surf.Sci, 255(11) (2009) 5869-5875.
[20] Shanefield D J, Organic Additives and ceramic processing, Kluwer Academic Publishers, Boston (1996) XIV, pp.316.
[21] Murugadoss G, J. Lumin, 130(11) (2010) 2207-2214.
[22] Lubos Jankovic, Nano Letters, 6(6) (2006) 1131.
[23] Meulenkamp EA, J. Phys. Chem B, 102 (1998) 5566.
[24] Helmut Kronmuller and Stuart Parkin (Eds.), Handbook of Magnetism and Advanced Magnetic Material, London: Wiley-Blackwell (2007). ISBN: 978-1-119-16713-6
[25] Nielsen K, Bauer S, L¨ubbe M, Physica Status Solidi A Appl Res, 203(14) (2006) 3581-3596.
[26] Akyol M and Bayramoğlu, J Hazard Mater, 124(1-3) (2005) 241-246.
[27] Gao J, Luan X, Wang J, Wang B, Li K, Li Y, Kang P and Han G, Desalination, 268 (2011) 68–75.
[28] Hermann, J.M. Catal. Today, 24 (1995) 157–164.

CITE AN ARTICLE

Vijayakumar, G., Bhoopathi, G., & Hilary, J. L. (n.d.). STRUCTURAL, OPTICAL AND PHOTO CATALYTIC PROPERTIES OF PVP ENCAPSULATED Ni2 Substituted ZnS NANOPARTICLES BY MODIFIED CO-PRECIPITATION METHOD. *INTERNATIONAL JOURNAL OF ENGINEERING SCIENCES & RESEARCH TECHNOLOGY*, *7*(3), 88-96